JOURNAL OF GEOPHYSICAL RESEARCH, VOL. 112, D13205, doi:10.1029/2006JD008099, 2007

Wintertime aerosol characteristics over the Indo-Gangetic Plain (IGP): Impacts of local boundary layer processes and long-range transport

Vijayakumar S. Nair,[1] K. Krishna Moorthy,[1] Denny P. Alappattu,[1] P. K. Kunhikrishnan,[1] Susan George,[1] Prabha R. Nair,[1] S. Suresh Babu,[1] B. Abish,[1] S. K. Satheesh,[2] Sachchida Nand Tripathi,[3] K. Niranjan,[4] B. L. Madhavan,[4] V. Srikant,[4] C. B. S. Dutt,[5] K. V. S. Badarinath,[6] and R. Ramakrishna Reddy[7]

Received 4 October 2006; revised 26 February 2007; accepted 28 March 2007; published 6 July 2007.

[1] The Indo-Gangetic Plain (IGP) encompasses a vast area, (accounting for ~21% of the land area of India), which is densely populated (accommodating ~40% of the Indian population). Highly growing economy and population over this region results in a wide range of anthropogenic activities. A large number of thermal power plants (most of them coal fed) are clustered along this region. Despite its importance, detailed investigation of aerosols over this region is sparse. During an intense field campaign of winter 2004, extensive aerosol and atmospheric boundary layer measurements were made from three locations: Kharagpur (KGP), Allahabad (ALB), and Kanpur (KNP), within the IGP. These data are used (1) to understand the regional features of aerosols and BC over the IGP and their interdependencies, (2) to compare it with features at locations lying at far away from the IGP where the conditions are totally different, (3) to delineate the effects of mesoscale processes associated with changes in the local atmospheric boundary layer (ABL), (4) to investigate the effects of long-range transport or moving weather phenomena in modulating the aerosol properties as well as the ABL characteristics, and (5) to examine the changes as the season changes over to spring and summer. Our investigations have revealed very high concentrations of aerosols along the IGP, the average mass concentrations (M_T) of total aerosols being in the range 260 to 300 μg m^{-3} and BC mass concentrations (M_B) in the range 20 to 30 μg m^{-3} (both ~5 to 8 times higher than the values observed at off-IGP stations) during December 2004. Despite, BC constituted about 10% to the total aerosol mass concentration, a value quite comparable to those observed elsewhere over India for this season. The dynamics of the local atmospheric boundary layer (ABL) as well as changes in local emissions strongly influence the diurnal variations of M_T and M_B, both being inversely correlated with the mixed layer height (Z_i) and the ventilation coefficient (V_c). The share of BC to total aerosols is highest (~12%) during early night and lowest (~4%) in the early morning hours. While an increase in the V_c results in a reduction in the concentration almost simultaneously, an increase in Z_{imax} has its most impact on the concentration after ~1 day. Accumulation mode aerosols contributed ~90% to the aerosol concentration at ALB, ~77 % at KGP and 74% at KNP. The BC mass mixing ratio was ~10% over all three locations and is comparable to the value reported for Trivandrum, a tropical coastal location in southern India. This indicates presence of submicron aerosols species other than BC (such as sulfate) over KGP and KNP. A cross-correlation analysis showed that the changes in M_B at KGP is significantly correlated with those at KNP, located ~850 km upwind, and ALB after a delay of ~7 days, while no such delay was seen between ALB and KNP. Back trajectory analyses show an enhancement in M_B associated with trajectories arriving from west, the farther from to the west they arrive, the more is the

[1]Space Physics Laboratory, VSSC, Trivandrum, India.
[2]Centre for Atmospheric and Oceanic Sciences, IISc, Bangalore, India.
[3]Department of Civil Engineering, Indian Institute of Technology, Kanpur, India.
[4]Department of Physics, Andhra University, Visakhapatnam, India.
[5]Indian Space Research Organisation Head Quarters, Antariksh Bhavan, Bangalore, India.
[6]National Remote Sensing Agency, Balanagar, Hyderbad, India.
[7]Sri Krishnadevaraya University, Anantapur, India.

0148-0227/07/2006JD008099$09.00

increase. This, along with the ABL characteristics, indicate two possibilities: (1) advection of aerosols from the west Asia and northwest India and (2) movement of a weather phenomena (such as cold air mass) conducive for build up of aerosols from the west to east. As the winter gives way to summer, the change in the wind direction and increased convective mixing lead to a rapid decrease in M_B.

Citation: Nair, V. S., et al. (2007), Wintertime aerosol characteristics over the Indo-Gangetic Plain (IGP): Impacts of local boundary layer processes and long-range transport, *J. Geophys. Res.*, *112*, D13205, doi:10.1029/2006JD008099.

1. Introduction

[2] Interaction of atmospheric aerosols with the solar and terrestrial radiations directly [*Charlson et al.*, 1992] and indirectly [*Twomey*, 1977] affects the radiation balance of the Earth-Atmosphere system and is thus believed to produce regional and global scale climate perturbations. Despite the concerted efforts over the last decade and several field campaigns, large uncertainties persist in the regional aerosol characteristics and their radiative impacts [*IPCC*, 2001], mainly due to the scarcity of data to describe the aerosol properties with adequate spatial and temporal resolution. This is greatly true for the Indian region [*Moorthy et al.*, 2005b]. In the recent years, there has been a flurry of observational campaigns, carried out over different parts of India, covering urban [*Babu et al.*, 2002b; *Tripathi et al.*, 2005a], coastal and continental regions of peninsular India [*Moorthy et al.*, 2005b], and oceanic environments [*Vinoj et al.*, 2004; *Moorthy et al.*, 2005a; *Satheesh et al.*, 2006]. Most of these campaigns, however, could not cover the vast continental landmass of India, comprising of the Indo-Gangetic Plain (IGP).

[3] The IGP encompasses a vast area from 21.75°N; 74.25°E to 31.0°N; 91.5°E and accounts for ~21% of the land area of Indian subcontinent. It is densely populated, accommodating ~40% of the Indian population. Highly growing economy and population over this region results in a wide range of anthropogenic activities ranging from biomass and fossil fuel burning, industries, transport, mining, urbanization, and agricultural activities. The eastern part of IGP is known as the coal belt of India, and has a cluster of coal-based thermal power plants (Figure 1), which are considered as the single significant emitters of particulate matter in this region (IGP) [*Prasad et al.*, 2006]. Other major sources of emission include a large number of small and medium industries, several of them using coal, scattered over the entire region, and open burning of litter and biofuels used for domestic cooking [e.g., *Reddy and Venkataraman*, 2002; *Girolamo et al.*, 2004]. Persistence of high aerosol optical depth (AOD) and large aerosol concentrations near the surface, as well as in the vertical column during winter months were reported recently at several locations in the region [*Jethva et al.*, 2005; *Ramana et al.*, 2004b; *Singh et al.*, 2004; *Prasad et al.*, 2006]. There were also a few studies using ground-based and satellite-derived data [*Jethva et al.*, 2005; *Girolamo et al.*, 2004; *Tripathi et al.*, 2005a; *Ramanathan and Ramana*, 2005; *Tripathi et al.*, 2006]. *Jethva et al.* [2005] have reported that the AOD values over the IGP are generally higher than those over other Indian regions for all seasons. The prevailing westerly winds, dry conditions during winter, the gradually dropping elevation and narrowing topography (with the Himalayas to the North and highlands of Bihar to the south) as we move from the west to east over the IGP [e.g.; *Girolamo et al.*, 2004; *Jethva et al.*, 2005] and the prevailing low, anticyclonic winds, are all conducive for advection from the west and confinement of aerosols over the central and eastern parts of the IGP. The low temperatures (with the minimum during night dipping as low as 0°C at many parts of the IGP in winter) and the low-wind speed (of <2 m s^{-1}) over the region inhibits vertical (convective) and horizontal mixing of aerosols produced at the surface due to shallow boundary layer and weak thermal convection [*Tripathi et al.*, 2005a]. Environmental and visibility degradation, formation of fog and disruption of day-to-day life is a consistent feature of every winter in many places of the IGP. As such, it is expected to have high aerosol loading for extended duration over this region. To characterize aerosols in this region and to understand their region specific, as well as more global aspects, a campaign mode observation was conducted over the IGP during the winter season of 2004, under the Indian Space Research Organization's Geosphere Biosphere Programme (I-GBP). For this we selected three sites lying in the IGP (central to eastern part) along the general direction of the prevailing winds and having similar topography and made collocated measurements of aerosol parameters. Details of the campaign and the results are presented in the following sections and the implications are discussed.

2. Site Description

[4] The main focus of the campaign was to characterize the near-surface aerosols, particularly the absorbing black carbon (BC), and to delineate the atmospheric processes that influence them during winter months. The campaign was for one full-month period (December 2004), during which simultaneous measurements were carried out from three stations within the IGP: viz, Kanpur (KNP, 26°24′N and 80°24′E; 142 m msl), Allahabad (ALB, 25°27′N & 80°44′E, 98 m msl), and Kharagpur (KGP, 22°31′N & 87°31′E; 28 m msl) lying from the west to east. These stations are marked in Figure 1, along with other neighboring major cities like New Delhi (DEL) and Kolkatta (KOL). Also shown in Figure 1 are the locations of major thermal power stations in India [www.mapsofindia.com/maps/india/thermalpowerplants.htm]. As can be see from it, >75% of them are clustered along the IGP. The sampling sites are selected such that they align almost along the direction of the prevailing winds, which arrive first at Kanpur, and proceed toward Allahabad and Kharagpur. The general topography and vegetation scenario are quite similar for all the three stations in the IGP, except that the mean altitude of the stations decrease gradually from west to east and the

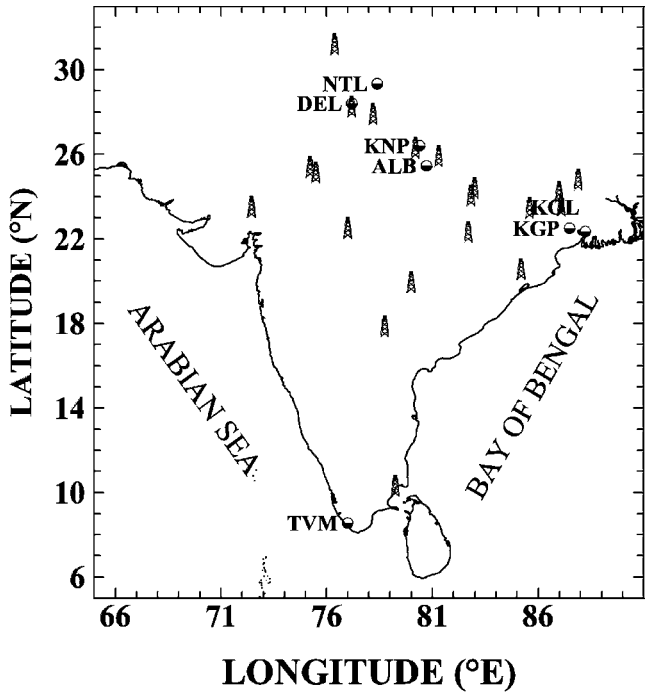

Figure 1. Location map showing the spatial distribution of the stations Kanpur (KNP), Allahabad (ALB), and Kharagpur (KGP), in the Indo-Gangetic Plain, where the campaign was carried out. A high-altitude station Nainital (NTL) in the central Himalayas and a coastal station Trivandrum (TVM) down south are also shown in the figure. The data from these stations are used for comparison. Locations of major cities such as New Delhi (DEL) and Kolkatta (KOL) are also marked. All these locations are identified by half-filled circles. In the same figure we have also shown the spatial distribution of major thermal power plants (coal based) in India represented by the stack symbol.

width of the valley (generated by the tall Himalayas to the north and the Highlands of Bihar to the south) narrows [e.g., *Girolamo et al.*, 2004; *Deepshikha et al.*, 2006; *Pant et al.*, 2007]. The time zone of all the stations, i. e., Kanpur, Allahabad, and Kharagpur, in the IGP is same, even though there is a longitudinal difference of ~7° between KNP and KGP. A short description of the sites are given below.

2.1. Kanpur

[5] Kanpur is an industrialized urban location with a population of over 4 million, situated in the IGP and the western most of the three stations considered in this work. It is located at ~250 km east of the mega city, New Delhi, (DEL in Figure 1) the capital of India with a population exceeding 10 million. The experimental site was at the Indian Institute of Technology Kanpur, which is on the northwest and mostly upwind side of the city. The major sources of pollution in the locality are automobiles, biomass burning (open burning in the winter and domestic cooking), and other industries [*Tripathi et al.*, 2006; *Tare et al.*, 2006]. Peak periods of traffic are from ~08:30 to 11:00 and from 17:30 to 20:00. Interannual and seasonal variation in aerosol characteristics and influence of dust storms over Kanpur has been studied by *Singh et al.* [2004] and *Dey et al.* [2005]. *Tare et al.* [2006] have reported the maximum anthropogenic contribution to the total extinction as ~83% during winter. Soil dust is not an important source of aerosols during the winter; however, it highly influences the aerosol characteristics during premonsoon and monsoon seasons [*Dey et al.*, 2004; *Singh et al.*, 2004; *Chinnam et al.*, 2006]. *Chinnam et al.* [2006] have identified three major sources of mineral dusts (mixed with anthropogenic pollutants) during summer months: (1) from Oman, (2) from southwest Asian basins, and (3) from Thar Desert in Rajasthan. Kanpur is mostly surrounded by vegetation and agricultural fields which are mainly vegetated during December month [*Deepshikha et al.*, 2006]. Recent studies by *Tare et al.* [2006] on the PM and BC emissions in the vicinity of Kanpur have shown three major sources: the soil derived, those form biomass burning, and those form gas-phase reactions products. The contribution of soil-derived components was significant in the coarse mode (diameter 0.95–10 μm); however, the other two sources dominated in the fine and accumulation modes.

2.2. Allahabad

[6] The city of Allahabad is located in south east part of Uttarpradesh State in the IGP, and has population of over >1 million, population density of ~17,000 km^{-2} and is located very close to Kanpur. The experimental measurements were carried out from the campus of the vast Allahabad University located in the periphery of the city; the site being ~50 m off a minor road in which two and three wheelers ply occasionally during the daytime. The traffic peaks from 09:00 to 11:00 and from 17:00 to 19:00 and comes to a near-standstill by ~20:00. The major roads are more than a kilometer away. Allahabad experiences wide range of temperature which goes as high as ~46°C in summer to a low as ~1°C in winter. Winds are predominantly from the northwest during the study period. The major source of emission in the locality is the automobiles. Other sources include scattered small and medium industries and tanneries. The usual practice of open fireplaces by local people during winter also adds to the air pollution on a large scale. The terrain is somewhat dusty with fine dust contributing significantly.

2.3. Kharagpur

[7] Kharagpur is a small town located toward the east coast of India and almost at the eastern end of the IGP. The town is ~80 km inland of the west coast of the BoB, ~100 km southwest of the city of Kolkatta (KOL in Figure 1 which has population of 4.5 million and population density of >100,000 km^{-2}) and is known for the vast campus of the Indian Institute of Technology (IIT). The other important institute is the Railway division offices. Other than these, the urban activities are rather minimal and the population in the town area of about 7-km radius is only ~180,000. The experiments were carried out from the terrace of the RRSSC (regional remote sensing service centre) building, located well inside the IIT campus. The small roads within the campus have occasional traffic due to cars and bikes. Buses, trucks, and other vehicles ply outside the campus, but not very large in number. The IIT campus is ~5 km west of the railway station, and the main railway line

Table 1. List of Instruments Used at Different Stations and the Parameters Measured

Instruments Used	Stations				
	KGP	KNP	ALB	NTL	TVM
Aethalometer	M_B	M_B	M_B	M_B	M_B
QCM	M_T	M_T	M_T	–	M_T
HVS	M_T	–	–	M_T	–
Tethered Balloon	Profile of temperature, pressure, relative humidity, wind speed, and wind direction up to ~1 Km	–	–	–	–

linking Kolkatta to the southern and southeastern parts of India passes about ~3 km away from the campus. Even though it has heavy traffic, it is basically an electrified track and only few diesel locomotives pass through it in any day. To the west, south, and north of the campus, are residential buildings. The traffic is not dense; peaks from ~09:00 to 11:00 and from 16:00 to 19:00 local time and by ~20:00 it is insignificant. Though the local anthropogenic activities and emissions are rather subdued, the state of Bihar, having large number of coal mines and heavy industries including steel plants lie to west and northwest of KGP.

2.4. Other Data

[8] In addition to measurements at these sites, regular measurements of aerosols (BC and total) were carried out at two stations lying well outside the IGP; Nainital (NTL, 29°20′N & 78°25′E), a high altitude (~2000 m MSL) station in the central Himalayas [*Pant et al.*, 2007]; and Trivandrum (TVM, 8°30′N & 77°E, 3 m msl), a coastal station far down south, where the winter conditions are felt with much reduced severity and fog conditions never occur [*Babu and Moorthy*, 2002]. These stations are also marked in Figure 1, and the data are used for comparison.

3. Instruments and Data

[9] Several instruments were used to characterize the aerosol properties at all the three stations. These are listed in Table 1 along with the parameters measured/retrieved. As can be seen from the table, an Aethalometer was used, one each at each of the stations, for continuous measurements of mass concentration (M_B) of aerosol BC, while for the total aerosols, 10-channel QCM cascade impactors were used. In addition, a single-stage high-volume sampler was used at Kharagpur, where the atmospheric boundary layer (ABL) parameters were also measured using a tethered balloon sonde. The measured ABL parameters are the altitude profiles of pressure (P, hPa), temperature (T, °C), relative humidity (RH, %), wind speed (U, ms^{-1}), and wind direction (θ, °) using sensors attached to the tethered, aerodynamically shaped balloon.

[10] The Aethalometer (Magee Scientific, USA) provides continuous and near real time estimates of M_B following optical attenuation technique [*Hansen et al.*, 1984]. This method has shown excellent agreement with other analytic techniques [*Allen et al.*, 1999; *Im et al.*, 2001] and has been widely used [*Babu et al.*, 2002; *Babu and Moorthy*, 2002; *Babu et al.*, 2004; *Tripathi et al.*, 2005a]. In a recent experiment *Hitzenberger et al.* [2006] have measured BC in a diesel exhaust dominated urban region of Vienna employing eight different methods (including the Aethalometer) and concluded that as far as the average values are concerned, all the methods agreed within their standard deviation and also that they all well captured the variations in the concentrations. Uncertainty in the measurements is of the order of 40 to 60 ng m^{-3}, for the set flow rate of 3 LPM (liter per minute) and time base of 5 min [*Babu et al.*, 2004]. Ambient air was aspirated from a height of 4 to 6 meter above the ground level at all the stations and the instruments were operated under identical conditions.

[11] Number of reports have appeared in the recent literature on the various methods for measuring elemental carbon (EC) or black carbon (BC, the light absorbing species of carbonaceous aerosols), their intercomparison, correction factors, accuracies, and error budget, under various ambient conditions [e.g., *Weingartner et al.*, 2003; *Schmid et al.*, 2005; *Hitzenberger et al.*, 2006]. Though *Hitzenberger et al.* [2006] observed a general agreement (within the respective standard deviation) between the different methods, for aged and well-mixed aerosols during summer, *Schmid et al.* [2005] found significant differences which are site-specific. Thus no method is generally accepted as a standard; the measured values are method-specific, depend on the type of the carbonaceous aerosol, and its fraction to the total aerosol mass [*Weingartner et al.*, 2003; *Hitzenberger et al.*, 2006]. Nevertheless, several concerted experiments have been conducted to compare the various techniques while measuring purely absorbing, purely scattering, and mixed aerosols: both in the nascent form (fresh, shortly after emission) and after aging and mixing with other aerosol types [e.g., *Weingartner et al.*, 2003; *Hitzenberger et al.*, 2006 and references therein]. Experiments such as "round robin" and "carbon shootout" were conducted [http://aerosol.web.psi.ch/workshop%20minute/min001_95r.pdf]. In several of these experiments, the Aetheolometer technique was compared with other methods such as the thermal, Integrating Sphere, etc. [e.g., *Hitzenberger et al.*, 2006], PSAP [*Schmid et al.*, 2005] and correction factors were recommended. *Weingartner et al.* [2003], while measuring different types of mixed aerosols and under varying concentrations, have suggested two correction factors: (1) the "C" factor that arises due to the amplification of the attenuation due to multiple scattering of light that passes through filter tape matrix and (2) the "R" factor arising due to "shadowing" by the particles that load the filter tape while sampling, which result in a decrease in the optical path in the filter and thus an underestimation of BC at higher particle loads. While the former tends to over estimate BC, the latter somewhat under estimates it and in a way compensates partly the effect of the former. On the basis of detailed analysis and several experiments, *Weingartner et al.* [2003] found that the "shadowing" effect and "R" factor is quite significant for "pure" soot particles, while almost negligible for aged atmospheric aerosols (which is a mixture). For the mixed aerosols, they estimated the C factor to be ~2.1. In our measurements we used an instrument factor 16.6 m^2 g^{-1} (given by the manufacturer). It accounts for a "C" factor (of 1.9) and an R factor derived from comparison with other techniques (T. Hansen, personal communication, 2005) so as to have the effective instrument factor of 16.6 m^2 g^{-1} at 880 nm. This is considered as "reasonably good in view of the fact that our sampling sites

were quite far from any strong sources (being well in the campus of education institutions) and away from main roads with significant traffic. Moreover, as will be seen subsequently, the BC share to the total aerosol mass was only ~10% in our study, so that it is not a BC dominated aerosol.

[12] Quartz Crystal Microbalance (QCM, model PC2, California Measurements Inc.) cascade impactor makes size resolved measurements of aerosol mass concentration ($\mu g\ m^{-3}$) in its 10 size bins, with 50% cut off diameters at >25 μm, 12.5, 6.4, 3.2, 1.6, 0.8, 0.4, 0.2, 0.1, and 0.05 μm for the stages 1 to 10, respectively. Measurements were made manually; at a flow rate of 0.24 liter min^{-1} and data are collected at an interval of 30 to 45 min with a sampling time of 5 min. Measurements were restricted to periods when the ambient RH was less than 75%, a condition prevailed at all the locations during most of the winter season. Following the error budgeting given by *Pillai and Moorthy* [2001], the error in the estimated mass concentration was in the range of 10 to 15% for each measurement.

[13] The single stage High Volume Sampler (Handi-Vol GH2000, Graseby Anderson, USA) collects aerosols on a 4-inch diameter quartz fiber substrate, which was preheated to 100°C, desiccated for 24 hr and tare weighed using a microbalance (Model AT 120, Mettler). After exposing the substrate to an ambient airflow, at the rate of 567 liter min^{-1} for 2 to 3 hr, the substrate was removed, desiccated, and weighed using the same microbalance in the room condition. The difference between the final and tare weights yielded the aerosol mass loading. Knowing the volume of air sampled, the mass concentration was estimated. Even though HVS and QCM measure total mass concentration using different techniques, their values were well correlated with a correlation coefficient of 0.78 and a regression slope of ~0.8, with the QCM values being lower. More details of the intercomparison procedures are available in the study of *Moorthy et al.* [2005b]. In addition, all the aerosol instruments deployed at the different locations were intercompared at a common location (New Delhi), by operating them collocated under identical conditions for 2 days (28 and 29 November 2004) and the consistency of results were established.

[14] The ABL measurements at Kharagpur during the campaign were made using a tethered sonde system (AIR USA). It consisted of an aerodynamically shaped balloon, payload, electric winch, and data acquisition system. Payload comprised of sensors for measuring P, T, RH, U, and θ (all symbols defined earlier) and the data are transmitted to the data acquisition system (at the ground) at every 20 s. The entire system had the capability to measure up to ~1.5 km. During the campaign period, on an average, four ascents were made per day. Each profiling needed about 45 to 60 min, when all the above ABL parameters were measured. From these measurements, other ABL parameters like potential temperature (T_P), boundary layer height (Z_i), and ventilation coefficient (V_c) were deduced. The measured temperature and pressure are used to compute the potential temperature T_P [*Stull*, 1988; *Ramana et al.*, 2004a]

$$T_P = T\left[\frac{1000}{P}\right]^{0.286} \quad (1)$$

where P is in hPa and T in °K. The altitude profiles of T_P are used to infer on the ABL characteristics.

4. General Meteorological Conditions

[15] The general meteorological conditions that prevail over the IGP during winter (December to February) comprise of dry conditions with nil or scanty rainfall, low-land temperatures (particularly during the nights), and a weak, low-level anticyclonic circulation. The mean winds [from NCEP (National Centers for Environmental Predication) data] at 850 hPa (Figure 2) were weak northerlies or northwesterlies over the IGP, while over the southern peninsula and adjoining oceans they were mostly easterlies with a northerly component. The prevailing circulation is conducive for confinement of aerosols over the IGP and coupled with the topographical features (discussed earlier) will favour an eastward advection. Day-to-day changes in the local ABL characteristics, on the other hand, have a strong bearing on the surface temperature and humidity. Monthly mean hourly values of temperature, relative humidity (RH), and winds near the surface were obtained from automatic weather stations operated near each of the observation sites. At all the three locations, temperature and RH showed significant diurnal variations. Diurnal temperature maximum occurs at around 14:30 LT, when RH is at its lowest value. Minimum temperature occurs at ~07:00, and around the same time RH reaches the diurnal peak. Both, the maximum and minimum temperature showed, on an average, a decrease from east to west across the IGP with KGP recording the highest maximum temperature of ~24.5°C, followed by Allahabad (~23°C) and Kanpur (~22.4°C). Similarly, the lowest minimum temperature (~4°C) occurred at KNP, followed by ALB (~8.6°C) and KGP (13.2°C). Winds are generally weak at all the stations being <~3 m s^{-1} at KNP and <2 m s^{-1} at KGP, on an average.

5. Results and Discussion

5.1. ABL Dynamics and Their Impacts on Aerosol Concentrations

[16] Two representative altitude profiles of potential temperature (T_P) are shown in Figure 3, for typical noontime (left panel) and typical nighttime (right panel) conditions. The various distinct regions are also marked in the figure. During daytime, Figure 3, left panel, shows the well-developed ABL comprising of a surface layer (SL) close to the ground where T_P decreases sharply with altitude, representing a super adiabatic regime. A ground-based inversion occurs at ~70 m marking the top of the SL above which T_p becomes nearly steady with altitude (due to turbulent mixing) representing an adiabatic lapse rate. This region of nearly constant T_p is the well-mixed layer (ML), the base of which is at the top of the SL. The height of the mixed layer or the ABL depth (Z_i) is the altitude of the base of the elevated inversion that separates the ML below from the entrainment zone above where the conditions are sub-adiabatic. In Figure 3 (left panel) this occurs at ~680 m and by convention, we define this as ABL height Z_i. During nighttime, land cools faster due to radiative cooling. Consequently the boundary layer structure changes, and a

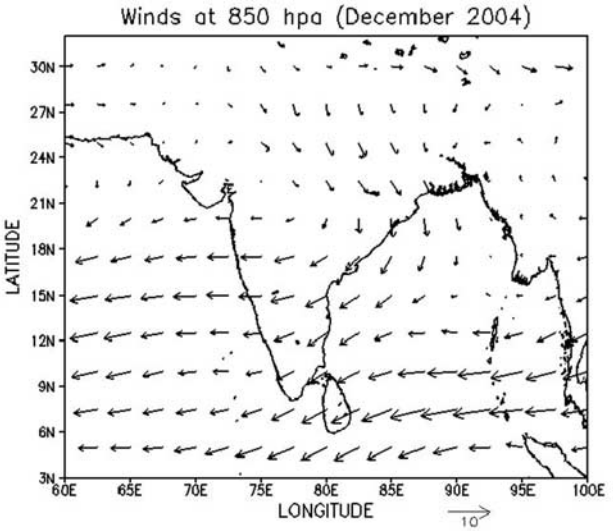

Figure 2. Mean prevailing winds at 850 hPa over the Indian region during December 2004 (from NCEP/NCAR reanalysis data).

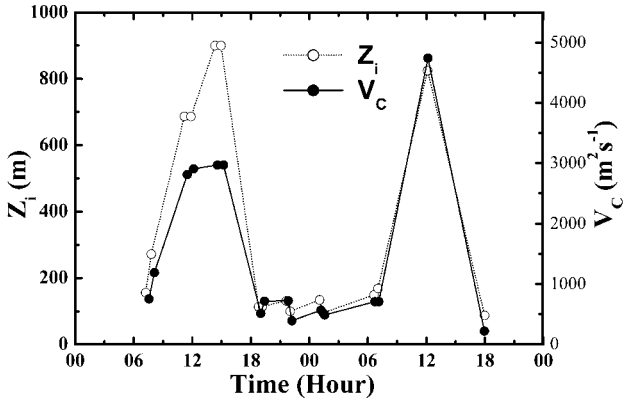

Figure 4. Diurnal evolution of the ABL at KGP as indicated by the variations of Z_i for 27–28 December 2004 (dashed line). The diurnal variation of ventilation coefficient (V_c) at KGP for the same period is shown by the solid line.

nocturnal stable layer forms above the ground. The profile of T_P in the right panel of Figure 3 shows the nocturnal potential temperature profile (at 21:39). The depth of the ground-based inversion (occurring at ~80 m) is clearly seen. The top of the ground-based inversion is the depth of the nocturnal boundary layer (NL). The region above the ground-based inversion is called the residual layer (RL). The ground-based inversion inhibits turbulent mixing within the NL.

[17] A typical example of the diurnal evolution of the ABL at KGP (for two representative days), as depicted by the variations of Z_i, is shown in Figure 4. The broad picture of the ABL evolution described above (i.e., the convectively driven daytime boundary layer and the stable nocturnal boundary layer) is clearly seen. During night (~18:00 to ~06:00 local time), the NL is quite shallow and Z_i remains at ~100–150 m. After the sunrise (which occurs at ~05:00 local time) the thermals gradually lift the inversion base, there by increasing the depth of the ABL. This is conducive for increased mixing of the atmospheric constituents in the mixed layer and a consequent redistribution of constituents in a greater atmospheric volume. The diurnal maximum in Z_i occurs in the afternoon at ~14:00, when the surface temperature also reaches around its peak value. In the evening, toward sunset, the ABL structure changes gradually to the nighttime conditions. As the ground-based inversion inhibits vertical transport of species from lower levels, the resulting confinement leads to an increase in

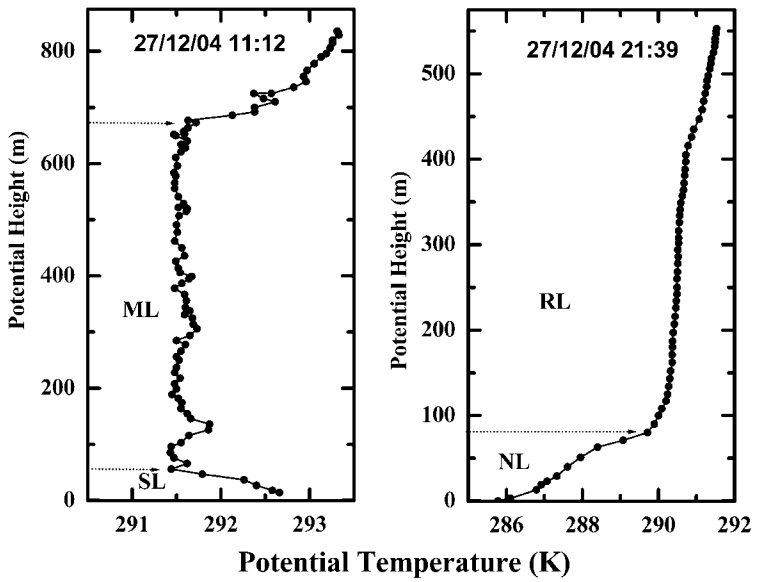

Figure 3. Profiles of potential temperature T_p depicting typical daytime conditions (on the left, obtained at 11:12 LT) and nighttime conditions (on the right, obtained at 21:39 LT). The different layers of the ABL are also marked: SL, surface layer; ML, mixed layer; NL, nocturnal (boundary) layer; and RL, residual layer. Details are given in the text.

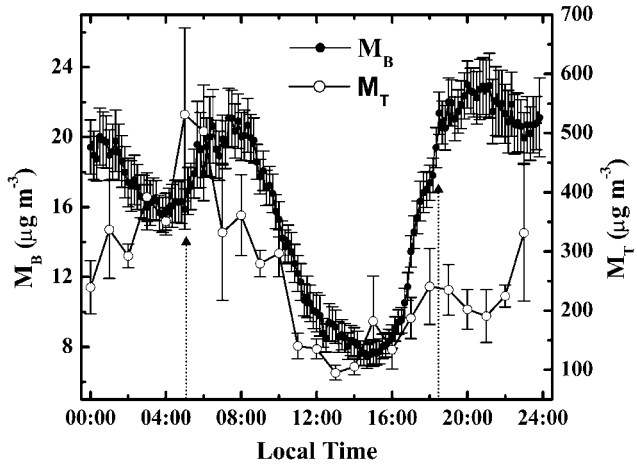

Figure 5. Diurnal variation of BC mass concentration (M_B) and total mass concentration (M_T) at KGP during December 2004. The local sunrise and sunset times (respectively, 05:05 and 17:25, for 15 December) are marked by the long vertical arrows on the abscissa.

their concentration. The above pattern repeats daily, even though its time evolution and the maximum value of Z_i differ.

[18] Ventilation coefficient (V_c) is an important parameter of the ABL that indicates the efficiency of the ABL to flush out the pollutants, including aerosols and thus has a significant role in pollutant dispersion and air quality studies. Ventilation coefficient is defined as the product of boundary layer height to the transport wind.

$$V_c = Z_i U_T \tag{2}$$

where U_T is the mean wind or transport wind, i.e., $U_T = \frac{1}{n}\sum_{1}^{n} U_i$ and U_i is the wind measured at each height and n is the number of levels within the ABL where the winds are measured. By virtue of the relation in equation (2), the ventilation coefficient accounts for vertical dispersion and (horizontal) advection of aerosols. The diurnal variation of V_c (Figure 4) is quite similar to Z_i. The increase in V_c is due to the increase in Z_i or U_T or both. As such, changes in the ventilation coefficient have similar effects on aerosol concentrations as that of the ABL height.

5.2. Aerosol Mass Concentrations

[19] Mass concentrations of composite (total) aerosols (M_T) and BC (M_B) showed strong diurnal variations. The average diurnal variation for December 2004 at KGP is shown in Figure 5. Here we have used the QCM measurements for M_T, primarily because these are available at closer temporal resolution, by grouping the individual measurements into hourly ensembles and averaging them over the whole month. Each hourly ensemble consisted of 30 to 60 samples with the early morning periods (04:00 to 07:00) having fewer samples than the daytime values owing to the restriction on the RH. The vertical bars are the standard deviation of the mean. For Aethalometer, we have averaged the data obtained at 5-min intervals over the month, so that the mean points are at 5-min interval and each point is an average of about 30 measurements.

[20] Both M_T and M_B show an afternoon minimum at around 14:00 and a nocturnal maximum, which occurs at ~20:00 for M_B and at around mid-night for M_T. Besides, there occurs a strong and short-lived peak shortly after sunrise, at around 05:30 for M_T and at ~07:30 for M_B. The local sunrise and sunset times (mean for December are at ~05:05, and ~17:15, respectively) are marked by the upward arrow on the abscissa. Similar diurnal variations were observed/reported also at KNP, and ALB in the north and TVM in the south [*Babu and Moorthy*, 2002; *Tripathi et al.*, 2005a], except that the time of occurrence of the early morning peak (in M_B) is shifted with the shift in the local sunrise time. The diurnal variation of M_T and M_B follows that of the ABL shown in Figure 4 and is attributed mainly due to the dynamics of the ABL. The deepening of the ABL during daytime, and the associated convective turbulence (Figures 3 and 4) thoroughly mix and redistribute aerosols, which were confined in the shallow NBL of the previous night, to greater vertical extent. This results in a dilution of their concentrations near the surface, which increases as the ABL deepens. The concentrations reach their diurnal low around the time when the ABL attains its maximum height. Toward evening the solar heating reduces and after the sunset, the thermals stop and mixed layer deforms to a shallow stable boundary layer near the surface and a residual layer aloft separated by an inversion in potential temperature (Figure 3, right panel), inhibiting vertical transport of aerosols. The resulting confinement leads to an increase in the species concentration near the surface. During morning, as the ABL evolves after sunrise, the strengthening thermals lift and eventually break the nighttime inversion causing the aerosols in the residual layer to mix with those near the surface leading to a sharp increase in the near-surface concentration, the effect being known as fumigation [*Stull*, 1988; *Fochesatto et al.*, 2001].

[21] Even though the dynamics of the ABL, described above, offers a general explanation to observed diurnal pattern of M_B, the finer aspects need a closer look. The sharp increase in M_B close to and after sunset cannot be attributed totally to the collapse of the ABL and the formation of NBL. Significant emissions from the local traffic, which peaks during the period ~1700 to ~1900 hr and the burning of fuels (both fossils and biofuels) for cooking and other household activities in the adjacent residential areas would be contributing to the sharp rise in M_B in the evening. As these BC particles are in fine size range, they would not add much to the total aerosol mass. In Figure 6 we examine the typical diurnal variation of BC mass fraction, F_{BC} (= M_B / M_T). It increases gradually from the lowest value (3.5% at ~05:00) to ~7% by 16:00 and then rather sharply to the peak value of ~12% attained by 20:00/21:00 hr. The domestic and vehicular emissions become insignificant or nil after 21:00 and the share of BC to total keeps on falling, This sharp increase in M_B and F_{BC} in the evening is thus due to local emissions of BC as described earlier. On the other hand, M_T, the total aerosol mass concentration, does not depend strongly on emissions from fuel usage and as such, its variations are not connected with this. From Figure 1, it appears that the emissions from the clustering thermal power plants might be contributing to M_T, but this needs to be confirmed. However, the sharp

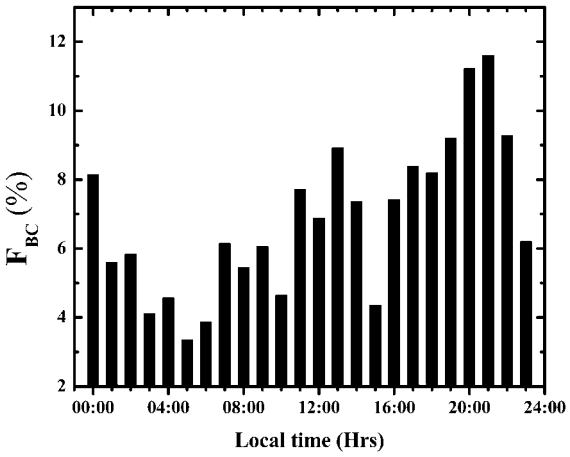

Figure 6. Diurnal variation of BC mass fraction.

morning peak in M_B after ~1 hr of sunrise is more due to fumigation because of the following observations.

[22] 1. The peak has a strong "sunrise time dependence" such that it occurs at all stations (covered in this study, as well as reported elsewhere and cited in the paper) about 60 to 90 min after local sunrise.

[23] 2. This peak occurs much before the rush traffic hours (which generally is from 08:30 to 11:00 for most of the locations in India, as whole India is in a single time zone and most of the establishments start functioning after 09:00 whether they are in KGP or TVM or KNP.

[24] The association between Z_i and M_B is examined quantitatively in Figure 7, which is a scatterplot of Z_i and M_B. The strong inverse relationship is obvious. A correlation analysis yields the coefficient $R = -0.89$, which is quite significant for the 27 points. The above observations show that the dynamics of the ABL and the changes in the local emissions strongly control the diurnal variation of the concentration of total and BC aerosols near the surface.

5.3. Day-to-Day Variations and Cross Correlations

[25] In addition to the impact on instantaneous aerosol concentrations, changes in ABL characteristics (Z_i and V_c) would affect the daily mean concentration and also might contribute significantly in causing day-to-day changes in the surface aerosol concentrations. Similarly changes in the transport wind U_T will result in corresponding changes in V_c. With a view to examine the day-to day changes in these parameters, we have plotted in Figure 8, the variations of the daily mean values of M_T and M_B with maximum BL height (Z_{imax}) for the day. In Figure 8 the values of M_T and M_B are shown according to the ordinate on the right. The very high concentrations (of both the total and BC aerosols) is strikingly seen and the mean values are about 5 to 8 times as high as those reported for other off-IGP continental locations in southern India [e.g., *Babu and Moorthy*, 2002]. This large abundance will be, at least partly, due to the special nature of this region, which is also the coal belt of India and has a cluster of coal-based thermal power stations. It is apparent from the same figure that the day-to-day variation of the aerosol concentrations are generally inversely related to those of Z_{imax}, even though not simultaneous always. For example, Z_{imax} was very low (<600 m)

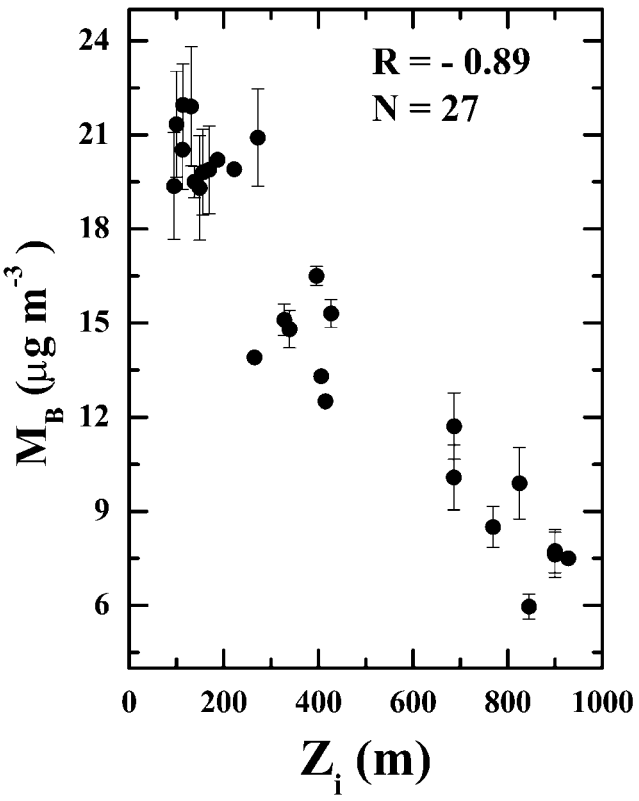

Figure 7. Scatterplot of BC mass concentration (M_B) against the corresponding Z_i. The correlation coefficients and number of points are also given in the figure.

during 15 to 18 December and M_T and M_B values were high during 16 to 19 December, indicating a delay in the response of daily mean M_B to the changes in Z_{imax}. To examine this we relied upon the cross correlations.

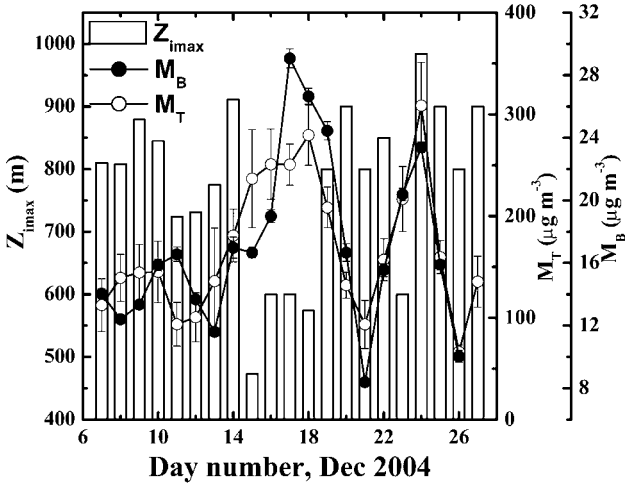

Figure 8. Day-to-day variations of the daily mean mass concentrations of total aerosols and BC (M_T and M_B) and the maximum boundary layer height (Z_{imax}) during December at KGP. Note that for M_B the ordinate scale is given on the right hand side.

Table 2. Cross Correlation Coefficients of Different Aerosol Parameters With the ABL Height for Different Lags

Lag in Days	Daily Mean M_T	Daily Mean M_B
0	−0.33	−0.33
1	−0.63	−0.65
2	−0.33	−0.56
3	0.02	0.01

[26] Association of two time series $x(i)$ and $y(i)$ having delay τ is studied using a standard statistical method, normalized cross correlation (NCC), the coefficient of which is defined as,

$$r(\tau) = \frac{\sum_i [x(i) - \overline{x}][y(i-\tau) - \overline{y}]}{\sqrt{\sum_i [x(i) - \overline{x}]^2}\sqrt{\sum_i [y(i-\tau) - \overline{y}]^2}} \quad (3)$$

where $\overline{x}$ and $\overline{y}$ are the means of two series, respectively, n is the total number of data points (number of days in the present case) and τ is the delay or lag in time for $y(i)$ to follow the variations in $x(i)$ and it could range from 0 to $n - 1$. Cross correlation with zero lag will give the normal correlation coefficient.

[27] Cross-correlation coefficients of M_B and M_T with Z_{imax} were calculated for different values of τ, from 0 to 3 days, in steps of 1-day and the results are summarized in Table 2. It is seen that the cross correlations increase, from a moderate value for 0-day lag, to the peak (with correlation coefficient ~−0.65) for a one-day lag; for both M_T and M_B. Subsequently, the coefficients drop down rapidly. Thus the changes in Z_{imax} influence mostly the daily mean aerosol concentrations of the next day.

[28] Unlike the case with Z_{imax}, it was observed that M_B and M_T responded faster to changes in the ventilation coefficient V_c, with maximum cross correlation obtained for 0 lag. In Figure 9 we have shown a scatterplot of M_B versus computed values of maximum V_c for all the 22 days. The scatterplot yields a close relationship, which is linear in log-log scale, implying a relationship of the form

$$M_B = M_{B0}(V_c)^{-\mu} \quad (4)$$

where M_{B0} represents the surface BC concentration for zero ventilation coefficient and μ is an index that determines the rate at which the BC decreases due to the increase in V_c. In Figure 9, almost all the points lie close to the regression line and yield a correlation coefficient of −0.85 except those on 21 and 22 December (identified in the figure). The correlation improves (with a coefficient of −0.95) if these two points are removed from the lot. The reason for this is examined separately in a later section in terms of change in the air mass type.

5.4. Spatial Distribution

[29] Spatial heterogeneity is the hallmark of aerosols and is the consequence of the distributed nature of the sources and sinks, as well as the long-range transport from far-off locations. This heterogeneity is important while developing regional models for estimating aerosol radiative forcing. Besides, examining the spatial distribution of aerosols help in understanding whether the features seen are purely local, regional, or synoptic. With these intentions we have examined the aerosol data collected at the three stations KNP, ALB, and KGP and also compared the features with those at other locations. The station KNP is located ~190 km northwest of Allahabad and ~850 km northwest of Kharagpur and all these stations lie almost along the direction of the prevailing wind as can be seen from Figures 1 and 2.

[30] A preliminary examination revealed that the day-to-day variations in M_B and M_T at these stations are quite similar in nature, though do not go one-to-one. With a view to quantifying the association, cross-correlation analysis was performed, with different lags up to 8 days. Results, in Figure 10, show that the cross-correlation coefficient initially decreases with the lag and then peaks sharply (with values in the range 0.5 to 0.6) for a lag of 6 to 7 days, for the data at KGP with respect to those at KNP. The coefficients are significant at $P = 0.09$. Similar results are seen with ALB also, but the correlations are weaker. On the other hand, the cross-correlation coefficients between KNP and ALB peaks (~0.6) for zero day lag and falls off for longer lags. This indicates the role of a common mechanism in producing a significant part of the day-to-day variations at these IGP stations. The weaker correlation between Allahabad and KGP might be arising due to the higher local anthropogenic contribution at that location (as seen later in section 5.6). In Figure 11, we show the temporal variations of daily mean (average) values of M_B at KNP and KGP, with those at KGP delayed by 7 days. Considering the parameters being compared and the type of variations they can have at any location, the observed association is very good. This suggests at least two possibilities: (1) advection and (2) movement of the particular meteorological condition that favors buildup of aerosols at KNP to ALB and KGP along the prevailing winds. As the prevailing winds, arrive at KNP much before than that at KGP, it is possible that advection is playing a role. Aircraft measurements of the altitude profiles of M_B at KNP during the winter of 2005

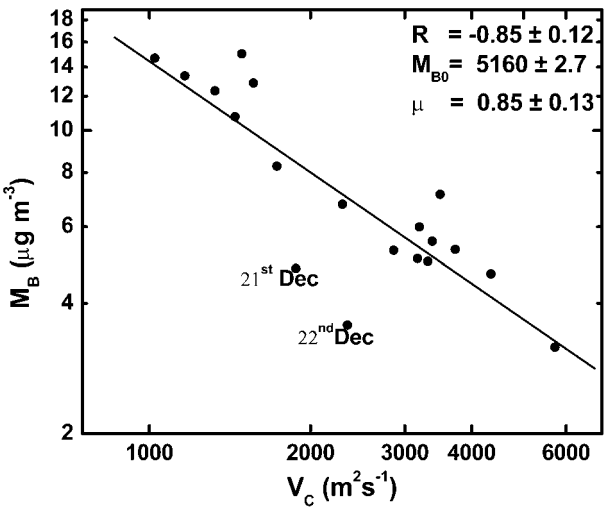

Figure 9. Scatterplot of noontime M_B against the corresponding V_c in a log-log scale. The points corresponding to 21 and 22 December are shown separately. The correlation coefficient R and parameters of equation (4) are also given in the figure.

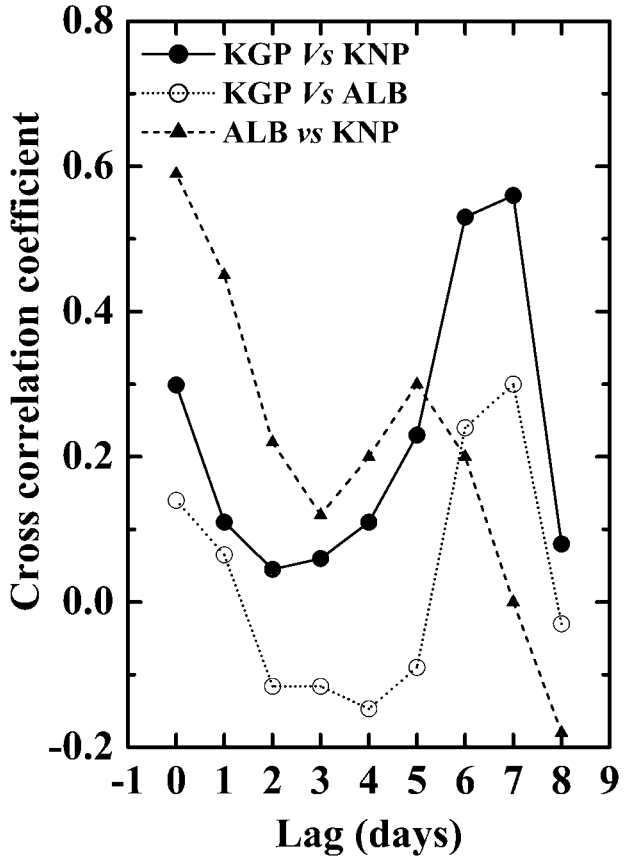

Figure 10. Variation of the cross-correlation coefficient of M_B with the lag-length in days for the variations at KGP, with respect to those at Kanpur (KNP) (solid line joining filled circles) and Allahabad (ALB) (dotted line joining unfilled circles). The same for ALB with respect to KNP is shown by the dashed lines joining the filled triangles.

[*Tripathi et al.*, 2005b] have shown the presence of elevated layer of BC, above the ABL (~900 m). If such layers occur, then advection becomes all the more important. In view of this, we examined the air mass trajectories ending at KGP. The second possibility is examined separately.

5.5. Role of Long-Range Transport

[31] Seven-day, isentropic back trajectories were computed for KGP for all the days of December 2004 using the HYbrid Single Particle Lagrangian Integrated Trajectory (HYSPLIT) model of National Oceanic and Atmospheric Administration (NOAA; *Draxler and Rolph*, 2003) for an altitude of 500-m AGL, which is well within the daytime ABL. The 7-day period was chosen in view of longer residence time (of >1 week) of fine aerosols during dry seasons, due to the lack of wet removal mechanisms, the low-wind speed (<2 ms^{-1}) and stable meteorological conditions. The mass plot of these trajectories, in Figure 12, shows advection pathways originating from local as well as far off locations on different days. A careful examination showed that these could be grouped as below:

[32] 1. West Asia: Where the trajectories originate from the west Asian regions 7 days before arriving KGP, and travel along the NW India and over the IGP (almost parallel to the Himalayan orography) before reaching KGP. All such cases are grouped and shown in the bottom panel of Figure 13.

[33] 2. IGP: Where the trajectories travel much less distances; are confined mostly to the east of 70°E (prior to 7 days of arriving at KGP) and travel across IGP as shown in the middle panel of Figure 13, and

[34] 3. Local: Where the trajectories are confined to the local region, not extending more than 5° in longitude to the west of KGP, as shown in the top panel of Figure 13.

[35] Examining the daily mean values of M_B and M_T in terms of these trajectory groups, it is seen that on all days when the concentrations showed an increase at KGP, the trajectories fell either of the first two groups. On the other hand, when the trajectories were of group 3, the concentrations tend to be lower. The mean values of M_B, which is a better tracer of the air mass movement owing to its lighter

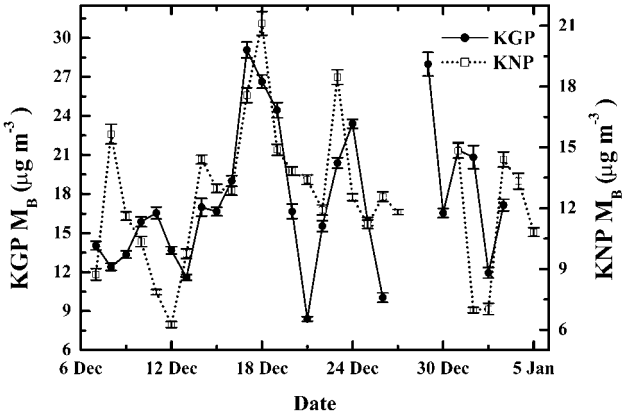

Figure 11. Comparison of the day to day variations of M_B at KNP with those at KGP, with the dates shifted by 7 days for KNP (for example, the points corresponding to 10 on the abscissa represents the data for Dec 10 at KGP and Dec 3 at KNP). The close similarity is worth noticing.

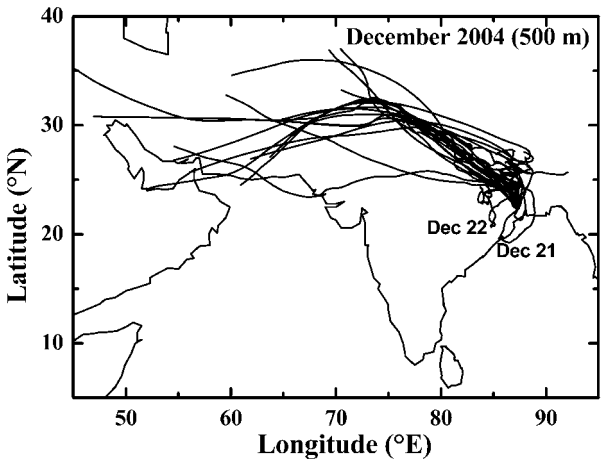

Figure 12. A mass plot of the 7-day back trajectories, arriving at 500 m over KGP for all the days of December 2004. Data generated using the HYSPLIT model.

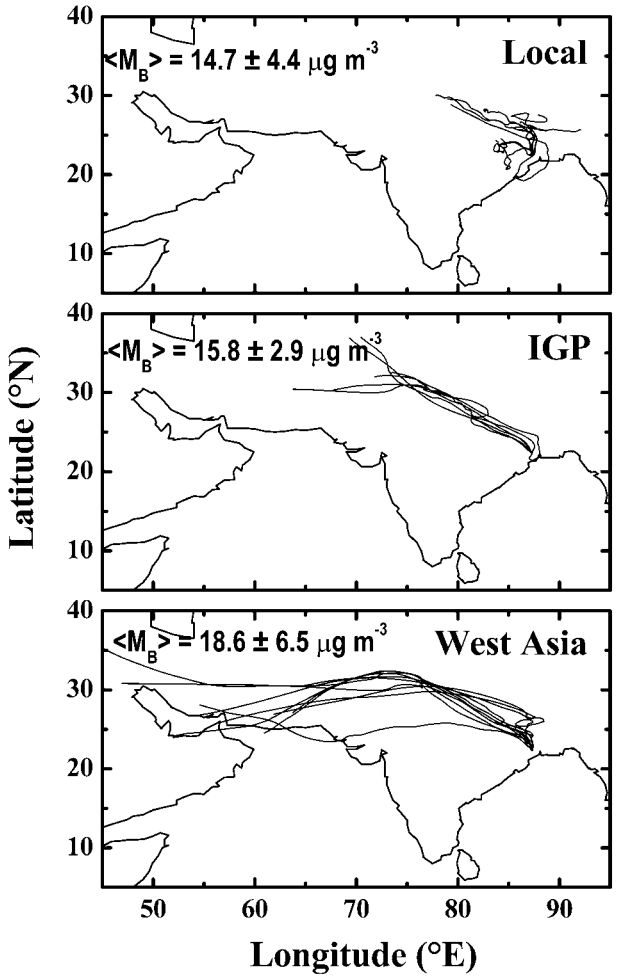

Figure 13. Trajectories shown in Figure 12, but separated depending on the extent of their land travel. Panels from top to bottom have the trajectories originating for locations increasingly farther westward/northwestward from KGP and KNP. The mean BC mass concentration in each case is also shown in the respective panels.

mass and longer life time than the composite (total) aerosols, for each trajectory group is estimated and is given in the corresponding panels of Figure 13. It is readily seen that the concentrations gradually increase as the trajectories travel more and more to the west, such that the mean M_B for the West Asian group is almost 50% higher than that for the local group. This strongly suggests that advection might be playing an important role in modulating the aerosol concentration and causing the day-to-day changes.

[36] Now we examine the second possibility of movement of the particular meteorological condition favoring confinement or buildup of aerosols. Examination of the individual trajectories in each panel of Figure 13 reveal that the trajectories of the west Asian panel (bottom most in Figure 13) belong to 10,11, 15 to 19, 22, and 23 December, 2004 and it is during the above periods that the aerosol concentrations show significant oscillations (increasing and then decreasing) about the mean level (Figure 11). On these days the maximum ABL height (Z_{imax}, Figure 8) is much lower than that for the adjacent days, even though no significant decrease in the maximum temperature is seen at KGP on these days. During the period 14 to 18 and 22 to 24, fog conditions were reported at stations like KNP and DEL. It is possible that the cooler air mass (from the northwest regions, where the minimum temperature drop close to 0°C on several nights during winter), propagates eastward and is responsible for the shallower ABL at KGP, despite the local conditions were not much different from the other days. For this we examine the ABL profiles on these days at KGP, a typical case is shown in Figure 14 for 16 December 2004. The bottom panel shows the profile close to local noon, while the top panel shows the afternoon profile. The very shallow nature of the ABL ($Z_i \sim 300$ m) and the highly subadiabatic variation above clearly indicates the advection of a cold air mass. Consequently, a very shallow nocturnal boundary layer formed early in the afternoon hours (top panel of Figure 14), well before the local sunset. The above observations thus suggest that both the processes, long-range transport of aerosols from the west and/or the movement of the cool meteorological front from the west to east would be responsible for the day-to-day changes in the aerosol concentrations. A well-planned experimental study is needed to quantify the role of each. In this context it may be noted that based on lidar, surface aerosols concentration, and columnar optical depth meas-

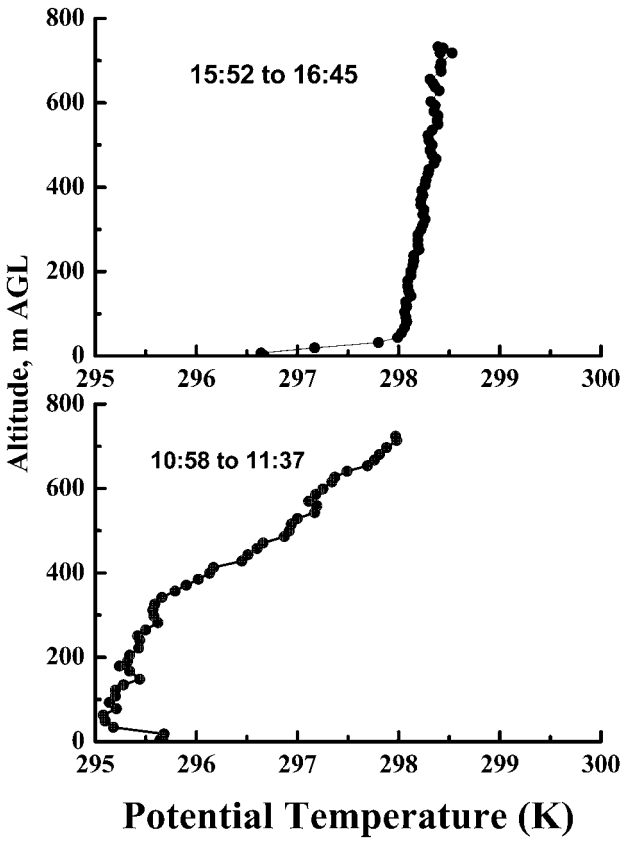

Figure 14. Thethersonde derived potential temperature profile for 16 December 2004 around the noon (at the bottom) and in the afternoon (top) showing, respectively, the suppression of convection and early onset of the nocturnal layer associated with advection of cold air mass.

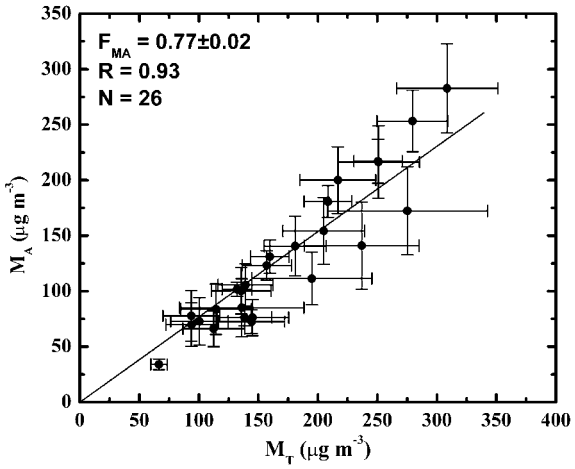

Figure 15. Scatterplot of the accumulation mode mass concentration (M_A) versus the total mass concentration (M_T) as derived from the QCM data at KGP.

urements from KGP during the same period, *Niranjan et al.* [2006], even though they did not see the signature of elevated layers at KGP in the lidar data during night, reported an increase in the columnar AOD (aerosol optical depth) during the same period when the surface concentrations showed the increase. Thus we infer that both the mechanisms would be contributing in producing the observed day-to-day changes.

[37] While examining the association between M_B and V_c in section 5.2, it was noticed that the correlation improved significantly (from -0.85 to -0.95), when the two points corresponding to 21 and 22 December were excluded. In other words, these 2 days behaved rather differently from the rest of the lot. The back trajectories for these days, identified in the trajectory group (Figure 12), show that on these days the advection was from the east coastal regions unlike the other days when the trajectories were directed from the interior landmass and was confined to rather short spatial extent.

5.6. Accumulation Mode Mass Concentration (M_A)

[38] The accumulation mode regime of aerosols ($\sim$0.1 to 1.0 μm) has significance as this size range is most efficient for scattering in the visible and near infrared. Therefore aerosol chemical components that reside within the accumulation mode will have a significant impact on the scattering/extinction properties of the total aerosol. Moreover, this mode is mostly attributed to anthropogenic sources and has considerable health implications. From the QCM measurements, mass concentration of the accumulation mode (M_A) aerosols was obtained by adding the mass concentrations from the stages 7 to 10. Mass fraction of M_A (F_{MA}) to the total aerosol mass is obtained from the slope of the scatterplot of M_A against M_T as shown in Figure 15 for KGP. It is found that at KGP M_A contributes $\sim$77% to M_T. Similar analysis for KNP [*Tripathi et al.*, 2006] and ALB yielded values of F_{MA} respectively as 74 and 90%. The comparatively high dominance of anthropogenic aerosols at Allahabad is possibly due to the large number of thermal plants and other industries around that region as described in section 2. This dominance of local source effects might be leading to the rather low response of aerosols there to long-range transport and the weaker correlations seen in Figure 10 and section 5.4.

5.7. BC Mass Fraction

[39] The mass fraction of BC (F_{BC}) to the total aerosols has a strong say on the aerosol absorption properties and the single scattering albedo (SSA) and is important in estimating the radiative impacts of aerosols [*Babu et al.*, 2004]. For a polluted marine aerosol model, they have shown that the atmospheric forcing efficiency due to aerosols (change in forcing per unit change in AOD) increases from 15 W m^{-2} for F_{BC} = 0.5%, to $\sim$65 W m^{-2} for F_{BC} = 5% and to $\sim$100 W m^{-2} for F_{BC} = 10%. From the collocated measurements of M_T and M_B, F_{BC} was estimated for each observation day and the monthly means are determined separately for KNP, ALB, and KGP and are shown in Figure 16. Side by side, we have also given the values obtained for Nainital in central Himalayas and Trivandrum (tropical coastal station) for the same period for comparison. It is interesting to note that over the IGP, BC contributes about 10% to the total aerosol mass and interestingly the share at the coastal station TVM also is about the same. Only at NTL, the share reduces to $\sim$5%, attributed to its elevated and remote nature and highly subdued human activity. It is also significant to add that the mass concentration of total aerosols at all the IGP stations are 5 to 10 times higher than the values seen at Trivandrum or in the southern peninsula [*Moorthy et al.*, 2005b], implying the persistence of large amount of BC over the IGP regions. This adds to the environmental and health implications. At this juncture we compare the F_{BC} of the present observations with other estimates made for different Indian regions. From an urban location Bangalore [*Babu et al.*, 2002] reported a value of 11.3%, while from a remote island location, Port Blair in the Bay of Bengal [*Moorthy and Babu*, 2006] have observed BC to contribute to 5.6% to the total aerosol mass. During INDOEX *Ramanathan et al.*, 2001 reported that BC contributes nearly

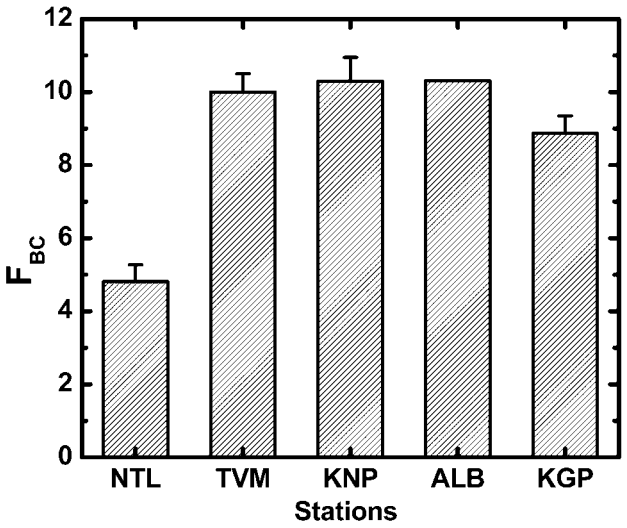

Figure 16. BC mass fraction (F_{BC}) over the IGP stations, compared with that at Nainital (NTL) and Trivandrum (TVM) for December 2004.

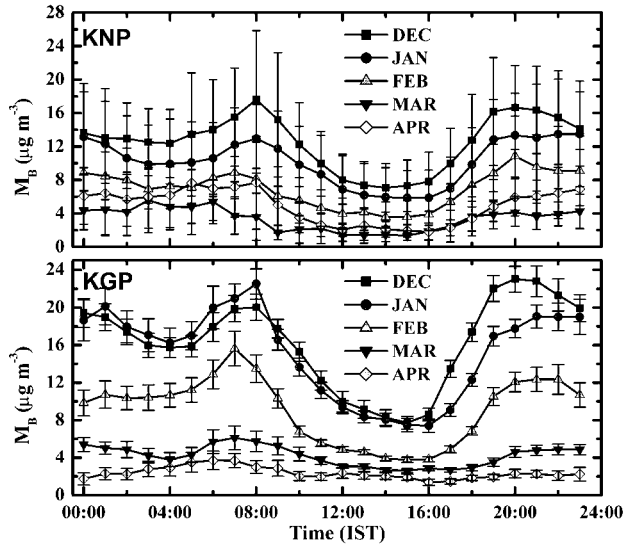

Figure 17. Monthly mean diurnal variations of M_B at KNP (top panel) and KGP (bottom panel) beyond the campaign period. Note the gradual decrease in the concentrations and the amplitude of diurnal variation at both the stations.

14% to the total fine aerosol mass concentration and 11% to the total mass concentration. All this point out that except at far and remote locations, and irrespective of the total loading, BC contributes to nearly 10% over most of the Indian regions during winter and this has significant implications to the radiative forcing [*Babu et al.*, 2004].

5.8. Characteristics Beyond Winter

[40] The Aethalometer measurements were continued beyond the campaign period at KGP and KNP until April 2005 primarily because they needed marginal attention. These data are examined to understand the changes in BC characteristics (which would be representative of the general characteristics of aerosols over the IGP) as the season changes. The (monthly averaged) diurnal variations of M_B are shown in Figure 17, for KNP (in the top panel) and KGP (bottom panel). The vertical lines through the points are the standard deviation of the mean. It can be noticed that

[41] 1. The nature of the diurnal variations remains more or less the same over the entire period and is similar, both at KGP and KNP. However, the absolute concentration and the amplitude of the diurnal variation decrease from December to April at both the stations.

[42] 2. The changes are more pronounced at KGP than at KNP.

[43] 3. The rate of decrease in M_B as the season progresses appears to be different at the two stations and this would be attributed to the difference in the local activities.

[44] The variation of monthly mean M_B at KGP and KNP is shown in Figure 18. For the sake of comparison, we also include the monthly mean values of M_B for TVM, lying far off from the IGP and having totally different environmental characteristics. Even though BC concentration decreases continuously from December to April at all the three stations, the decrease is most pronounced at KGP while it is least pronounced at TVM. Interestingly, as summer conditions set-in, the concentrations at KGP fall below the values at TVM and KNP. At KNP, the concentrations decrease till March and then there is a weak increase, probably associated with the local activities such as burning of agrowaste. Despite all these, the substantial decrease in M_B is indisputable. As the rainfall in northern India is insignificant during the entire period (unlike at TVM, where some summer showers are experienced in April) this decrease could be attributed to changes in synoptic advection pathways as well as the rapid increase in dispersion and ventilation due to large increase in the thermal convections as the land temperatures rapidly increase at these stations as winter changes to spring and summer. The striking difference is the change in pathways of long-range transport at KGP can clearly be seen in the mass back-trajectory plots in Figure 19, where we have shown the trajectories for each month, estimated as explained earlier. (The trajectory for December is shown already in Figure 12 and not repeated). The trajectories, which were predominantly of western origin in December, continue so in January also, but from February onward, trajectories shift increasingly to southerlies, coming from over the Bay of Bengal and by April more than 50% of the days the trajectories arrive from the Bay. The increased influx of this cleaner oceanic air is, thus, a significant factor contributing to the rapid reduction in the aerosol (BC) concentrations over KGP. However, the inland station KNP showed occurrence of mixed trajectories, from west Asia as well as from the Arabian Sea (due west to the peninsula) and a clear picture could not be obtained. Detailed investigations are needed to understand the influence of this to more interior regions of the IGP.

6. Summary

[45] During an intense field campaign, extensive measurements of aerosol concentrations using collocated instruments and boundary layer parameters (using tethered balloon sonde) were made at three locations in the IGP, Kharagpur, Kanpur, and Allahabad. Spatiotemporal hetero-

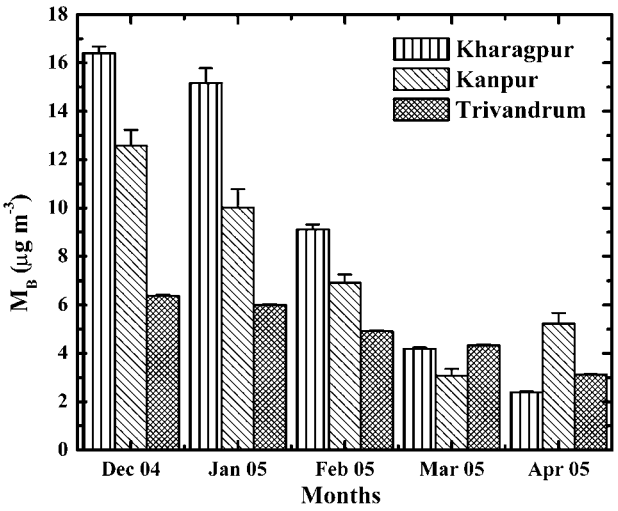

Figure 18. Variation of the monthly mean BC concentration at KGP and KNP for the period December 2004 to April 2005 being compared with similar variation at TVM, bringing out the spatial heterogeneity over large scales.

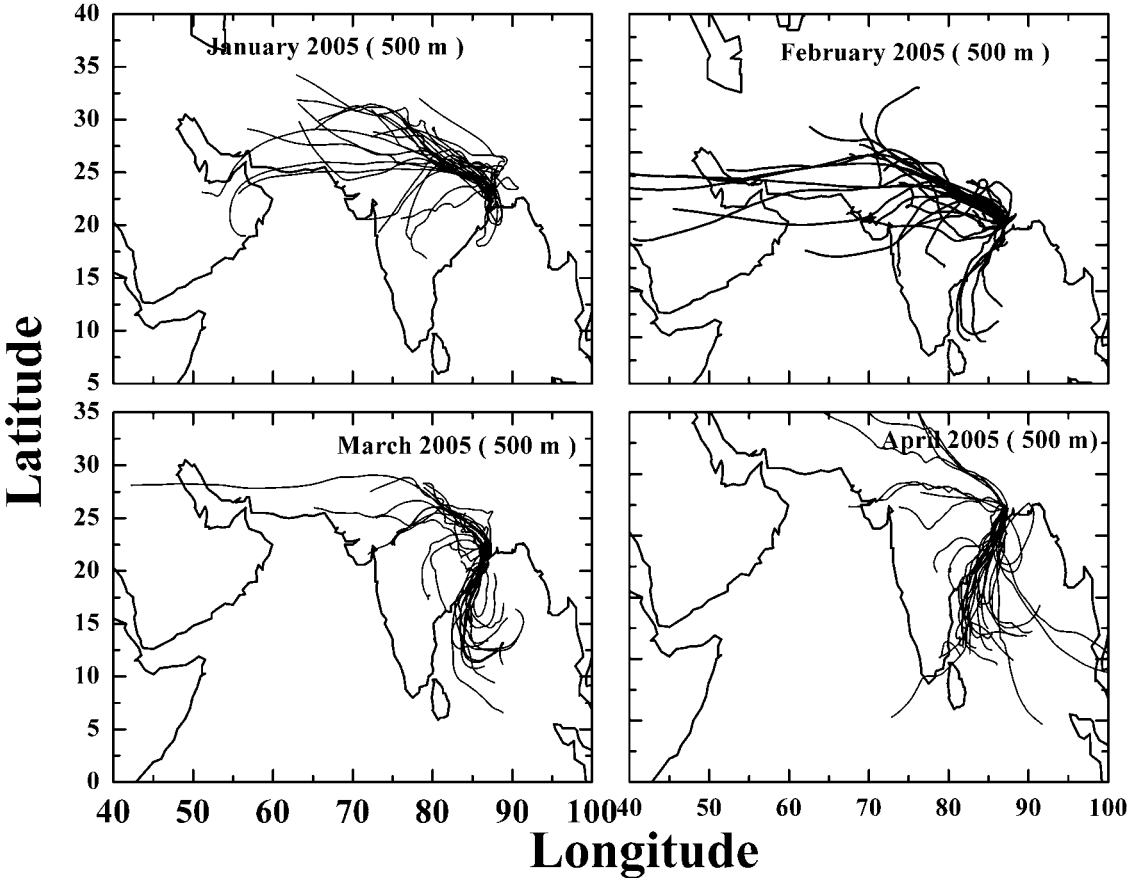

Figure 19. Mass plot of 7-day back trajectories (HYSPLIT) arriving over KGP at 500 m for the months January 2005 to April 2005. The gradual shifts in the trajectories from mostly westerlies to dominant easterlies as the season advances.

geneity of aerosols and its association with boundary layer process, synoptic scale circulations, and long-range transport during winter were examined. Our investigations have revealed that.

[46] 1. Mass concentrations of aerosols (total and BC) are significantly high (by nearly a factor of 5 to 10) over the IGP stations during winter, compared to the off-IGP locations.

[47] 2. Dynamics of the local atmospheric boundary layer strongly influences the diurnal changes in the concentrations of the total aerosols (M_T) and of aerosol BC (M_B). The variations of M_B and M_T are inversely correlated to those of the mixed layer height and the ventilation coefficient.

[48] 3. Besides the ABL dynamics, local emissions also contribute to the diurnal variations. These appear to contribute differently to total and BC aerosols so that the BC mass fraction is highest during evening and early night, while it is lowest in the early morning periods.

[49] 4. The accumulation mode aerosols contribute to 77, 74, and 90%, respectively, over KGP, KNP, and ALB.

[50] 5. The average BC mass mixing ratio is ~10% over all three locations and is comparable to that reported for other locations in the southern India. Viewed along with other published results, this shows that during winter season BC contributes nearly 10% to the total aerosol mass almost over entire India, except at high-altitude locations.

[51] 6. Cross-correlation analyses showed that the changes in M_B at KGP are significantly correlated with those at KNP and Allahabad (located ~850 km upwind), with a delay of ~7 days. No such delay was noticed between KNP and ALB.

[52] 7. Air back trajectory analysis showed an enhancement in M_B associated with advection from the west, the enhancement being more; the more trajectories go back to the west. This is attributed to either advection of aerosols from the west and/or the movement of meteorological conditions favoring confinement or buildup of aerosols (e.g., reduced vertical mixing during a cold air mass movement) from west to east.

[53] 8. As the winter conditions change to spring and summer, the concentrations decrease rapidly at KNP and KGP due to the combined action of the increased vertical mixing and the changes in the prevailing wind direction.

[54] **Acknowledgments.** The work was carried out under the Geosphere Biosphere Program of Indian Space Research Organisation. The authors thank A Jeyaram, MD Behera, and other colleagues of the regional remote sensing service center at Kharagpur (RRSSC-K) for supporting the campaign and in data collection beyond the campaign period. Several useful suggestions from the reviewers have helped to improve the paper.

References

Allen, G. A., J. Lawrence, and P. Koutrakis (1999), Field validation of a semi-continuous method for aerosol black carbon (Aethalometer) and

temporal patterns of summertime hourly black carbon measurements in south-western PA, *Atmos. Environ.*, *33*, 817–823.

Babu, S. S., and K. K. Moorthy (2002), Aerosol black carbon over tropical coastal station in India, *Geophys. Res. Lett.*, *29*(23), 2098, doi:10.1029/2002GL015662.

Babu, S. S., S. K. Satheesh, and K. K. Moorthy (2002), Aerosol radiative forcing due to enhanced black carbon at an urban site in India, *Geophys. Res. Lett.*, *29*(18), 1880, doi:10.1029/2002GL015826.

Babu, S. S., K. K. Moorthy, and S. K. Satheesh (2004), Aerosol black carbon over Arabian sea during inter monsoon and summer monsoon seasons, *Geophys. Res. Lett.*, *31*, L06104, doi:10.1029/2003GL018716.

Charlson, R. J., S. E. Schwartz, J. M. Hales, R. D. Cess, J. A. Coakley, J. E. Hansen, and D. J. Hoffman (1992), Climate forcing by anthropogenic aerosols, *Science*, *255*, 423–430.

Chinnam, N., S. Dey, S. N. Tripathi, and M. Sharma (2006), Dust events in Kanpur, Northern India: Chemical evidence for source and implications to radiative forcing, *Geophys. Res. Lett.*, *33*, L08803, doi:10.1029/2005GL025278.

Deepshikha, S., S. K. Satheesh, and J. Srinivasan (2006), Dust aerosols over India and adjacent continent retrieved using METEOSAT infrared radiance: Part 1. Sources and regional distribution, *Ann. Geophys.*, *24*(1), 37–61.

Dey, S., S. N. Tripathi, R. P. Singh, and B. Holben (2004), Influence of dust storm on the aerosol parameters over the Indo-Gangetic Basin, *J. Geophys. Res.*, *109*, D20211, doi:10.1029/2004JD004924.

Dey, S., S. N. Tripathi, R. P. Singh, and B. Holben (2005), Seasonal variability of the aerosol parameters over the Indo-Gangetic basin, *Adv. Space Res.*, *36*, 777–782.

Draxler, R. R., and G. D. Rolph (2003), HYSPLIT (Hybrid Single Particle Lagrangian Integrated Trajectory) model access (Available online at http://www.arl.noaa/gov/ready/hysplit.html).

Fochesatto, G. J., P. Drobinski, C. Flamant, D. Guedalia, C. Sarrat, P. H. Flamant, and J. Pelon (2001), Evidence of dynamical coupling between the residual layer and the developing convective boundary layer, *Boundary Layer Meteorol.*, *99*, 451–464.

Girolamo, L., T. C. Bond, D. Bramer, D. J. Diner, F. Fettinger, R. A. Kahn, J. V. Martonchik, M. V. Ramana, V. Ramanathan, and P. J. Rasch (2004), Analysis of multiangle imaging spectro-radiometer (MISR) aerosol optical depths over greater India during winter 2001–2004, *Geophys. Res. Lett.*, *31*, L23115, doi:10.1029/2004GL021273.

Hansen, A. D. A., H. Rosen, and T. Novakov (1984), The Aethalometer, an instrument for the real-time measurement of optical absorption by aerosol particles, *Sci. Total Environ.*, *36*, 191–196.

Hitzenberger, R., A. Petzold, H. Bauer, P. Ctyroky, P. Pouresmaeil, L. Laskus, and H. Puxbaum (2006), Intercomparison of thermal and optical measurement methods for elemental carbon and black carbon at an urban location, *Environ. Sci. Technol.*, 6377–6383.

Im, J. S., V. K. Saxena, and B. N. Wenny (2001), An assessment of hygroscopic growth factors for aerosols in the surface boundary layer for computing direct radiative forcing, *J. Geophys. Res.*, *106*, 20,213–20,224.

Intergovernmental Panel on Climate Change (2001), Climate Change 1994: Radiative Forcing of Climate, Report to IPCC From the Scientific Assessment Group (WGI), Cambridge Univ. Press, New York.

Jethva, H., S. K. Satheesh, and J. Srinivasan (2005), Seasonal variability of aerosols over the Indo-Gangetic basin, *J. Geophys. Res.*, *110*, D21204, doi:10.1029/2005JD005938.

Moorthy, K. K., and S. S. Babu (2006), Aerosol black carbon over bay of Bengal observed from an island location, Port Blair: Temporal features and long-range transport, *J. Geophys. Res.*, *111*, D17205, doi:10.1029/2005JD006855.

Moorthy, K. K., S. S. Babu, and S. K. Satheesh (2005a), Aerosol characteristics and radiative impacts over the Arabian Sea during the intermonsoon season: Results from ARMEX Field campaign, *J. Atmos. Sci*, *62*, 192–206.

Moorthy, K. K., et al. (2005b), Wintertime spatial characteristics of boundary layer aerosols over Peninsular India, *J. Geophys. Res.*, *110*, D08207, doi:10.1029/2004JD005520.

Niranjan, K., V. Sreekanth, B. L. Madhavan, and K. K. Moorthy (2006), Wintertime aerosol characteristics at a north Indian site Kharagpur in the Indo-Gangetic plains located at the outflow region into Bay of Bengal, *J. Geophys. Res.*, *111*, D24209, doi:10.1029/2006JD007635.

Pant, P., P. Hegde, U. C. Dumka, R. Sagar, S. K. Satheesh, K. K. Moorthy, and M. K. Srivastava (2007), Aerosol characteristics at a high altitude location in Central Himalayas: Optical properties and radiative forcing, *J. Geophys. Res.*, *111*, D17206, doi:10.1029/2005JD006768.

Pillai, P. S., and K. K. Moorthy (2001), Aerosol mass-size distributions at a tropical coastal environment: Response to mesoscale and synoptic processes, *Atmos. Environ.*, *35*, 4099–4112.

Prasad, A. K., R. P. Sing, and M. Kafatos (2006), Influence of coal based thermal power plants on aerosol optical properties in the Indo-Gangetic basin, *Geophys. Res. Lett.*, *33*, L05805, doi:10.1029/2005GL023801.

Ramana, M. V., P. Krishnan, S. M. Nair, and P. K. Kunhikrishnan (2004a), Thermodynamic structure of the atmospheric boundary layer over Arabian sea and the Indian Ocean during pre-INDOEX and INDOEX-FFP campaigns, *Ann. Geophys.*, *22*, 2679–2691.

Ramana, M. V., V. Ramanathan, I. A. Podgorny, B. B. Pradhan, and B. Shrestha (2004b), The direct observations of large aerosol Radiative forcing in the Himalayan region, *Geophys. Res. Lett.*, *31*, L05111, doi:10.1029/2003GL018824.

Ramanathan, V., and M. V. Ramana (2005), Persistent widespread and strongly absorbing haze over the Himalayan foothills and the Indo-Gangetic Plains, *Pure Appl. Geophys.*, *162*, doi:10.1007/s00024-005-2685-8.

Ramanathan, V., et al. (2001), Indian Ocean experiment: An integrated analysis of the climate forcing and effects of the great Indo-Asian haze, *J. Geophys. Res.*, *106*(D22), 28,371–28,398, doi:10.1029/2001JD900133.

Reddy, M. S., and C. Venkataraman (2002), Inventory of aerosol and sulphur dioxide emissions from India: I. Fossil fuel combustion, *Atmos. Environ.*, *36*, 677–697.

Satheesh, S. K., K. K. Moorthy, Y. J. Kaufman, and T. Takemura (2006), Aerosol Optical depth, Physical properties and Radiative forcing over the Arabian Sea, *Meteorol. Atmos. Phys.*, *91*, 45–62, doi:10.1007/s00703-004-0097-4.

Schmid, O., P. Artaxo, W. P. Arnott, D. Chand, L. V. Gatti, G. P. Frank, A. Hoffer, M. Schnaiter, and M. O. Andreae (2005), Spectral light absorption by ambient aerosols influenced by biomass burning in the Amazon Basin: I. Comparison and field calibration of absorption measurement techniques, *Atmos. Chem. Phys. Disc.*, *5*, 9355–9404.

Singh, R. P., S. Dey, S. N. Tripathy, and V. Tare (2004), Variability of aerosol parameters over Kanpur, northern India, *J. Geophys. Res.*, *109*, D23206, doi:10.1029/2004JD004966.

Stull, R. B. (1988), *An Introduction to Boundary Layer Meteorology*, Springer, New York.

Tare, V., et al. (2006), Measurement of atmospheric parameters during ISRO-GBP Land Campaign II at a typical location in the Ganga Basin: 2. Chemical properties, *J. Geophys. Res.*, *111*, D23210, doi:10.1029/2006JD007279.

Tripathi, S. N., S. Dey, V. Tare, and S. K. Satheesh (2005a), Aerosol black carbon Radiative forcing at an industrial city in northern India, *Geophys. Res. Lett.*, *32*, L08802, doi:10.1029/2005GL022515.

Tripathi, S. N., S. Dey, V. Tare, S. K. Satheesh, S. Lal, and S. Venkataramani (2005b), Enhanced layer of black carbon in a north Indian industrial city, *Geophys. Res. Lett.*, *32*, L12802, doi:10.1029/2005GL022564.

Tripathi, S. N., et al. (2006), Measurement of atmospheric parameters during ISRO-GBP Land Campaign II at a typical location in the Ganga Basin: 1. Physical and optical properties, *J. Geophys. Res.*, *111*, D23209, doi:10.1029/2006JD007278.

Twomey, S. A. (1977), The influence of pollution on the short-wave albedo of clouds, *J. Atmos. Sci.*, *34*, 1149–1152.

Vinoj, V., S. S. Babu, S. K. Satheesh, K. K. Moorthy, and Y. J. Kaufman (2004), Radiative forcing by aerosols over the Bay of Bengal region derived from shipborne, island-based, and satellite (Moderate-Resolution Imaging Spectroradiometer) observations, *J. Geophys. Res.*, *109*, D05203, doi:10.1029/2003JD004329.

Weingartner, E., H. Saathoff, M. Schnaiter, N. Strit, B. Bitnar, and U. Baltensperger (2003), Absorption of light by soot particles: Determination of the absorption coefficient by means of aethalometers, *J. Aerosol Sci.*, *34*, 1445–1463.

B. Abish, D. P. Alappattu, S. S. Babu, S. George, P. K. Kunhikrishnan, K. K. Moorthy, P. R. Nair, and V. S. Nair, Space Physics Laboratory, VSSC, Trivandrum – 695 022, India. (krishnamoorthy_k@vssc.gov.in)

K. V. S. Badarinath, National Remote Sensing Agency, Balanagar, Hyderbad – 500 037, India. (badrinath_kvs@nrsa.gov.in)

C. B. S. Dutt, Indian Space Research Organisation Head Quarters, Antariksh Bhavan, New BEL road, Bangalore – 560 094, India. (dutt_cbs@ isro.gov.in)

B. L. Madhavan, K. Niranjan, and V. Srikant, Department of Physics, Andhra University, Visakhapatnam – 530 003, India. (niranjankandula@hotmail.com)

R. R. Reddy, Sri Krishnadevaraya University, Anantapur – 515 003, India. (rajururreddy@gmail.com)

S. K. Satheesh, Centre for Atmospheric and Oceanic Sciences, IISc, Bangalore – 560 012, India. (satheesh@caos.iisc.ernet.in)

S. N. Tripathi, Department of Civil Engineering, Indian Institute of Technology, Kanpur – 208016, India. (snt@iitk.ac.in)